Analytical Methods

ROYAL SOCIETY OF CHEMISTRY

PAPER

View Article Online
View Journal | View Issue

Cite this: *Anal. Methods*, 2026, **18**, 2914

Avoiding and reducing microplastic false positives from dry glove contact

Madeline E. Clough, [a] Eduardo Ochoa Rivera,[b] Abbygail M. Ayala, [a] Rebecca L. Parham, [a] Joseph Pennacchio,[b] Henry E. Thurber, [c] Andrew P. Ault, [a] Ambuj Tewari [bd] and Anne J. McNeil *[ace]

To attenuate microplastics pollution, we first must quantify the number and types of microplastics found in the natural environment and identify their sources. Quantifying environmental microplastics requires distinguishing synthetic polymers from other naturally occurring species. Quality assurance and control measures – including wearing gloves when handling laboratory materials and samples – seek to reduce overestimating microplastic abundance. However, commonly used laboratory gloves release non-volatile residues, including stearate salts, that exhibit vibrational spectra similar to microplastics. In this work, we illustrate that dry surface contact with nitrile and latex laboratory gloves can cause overestimations of microplastics (mean 2000 false positives per mm^2) when using traditional library matching approaches. We recommend a nitrile cleanroom glove (mean 100 false positives per mm^2) to reduce contamination. For existing contaminated infrared and Raman spectral datasets, we outline workflows that differentiate between microplastics and stearate contamination from gloves. Applying these workflows to a case study of glove-contaminated environmental data, we illustrate that the proposed solutions reduce MP false positives at the smallest size ranges (<10 μm). By using this approach in conjunction with our included spectral libraries of stearate standards, researchers can address glove-based contamination in environmental datasets and provide more accurate estimates of environmental microplastic abundance.

Received 29th October 2025
Accepted 11th March 2026

DOI: 10.1039/d5ay01801c

rsc.li/methods

Introduction

Alongside the expanding production of synthetic polymers has come the unintended, yet significant, consequences of plastic pollution in the environment.[1–4] Plastics can degrade to create particles 1–5000 micrometres in size,[5,6] called microplastics (MPs),[7] which can travel between ecosystems and impact plant and animal health.[8–10] As reports of negative health effects related to MP pollution continue,[11–13] we must identify the major sources of MPs and their abundance in the environment to inform solutions.

Remediation and regulation to address MP pollution rely on researchers to accurately identify and quantify MPs across diverse matrices.[14,15] As plastic is ubiquitous in both laboratory and environmental settings, researchers have compiled strict quality assurance and quality control (QA/QC) measures to avoid unintentional contamination.[16–18] Recommendations include wearing cotton laboratory coats over synthetic textiles,[19–21] using glass or metal laboratory supplies rather than plastic,[22,23] guaranteeing purity of materials and surroundings,[24–26] and instituting procedural blanks to assess MP contamination in the sampling and analysis workflow.[27,28] These QA/QC measures minimize the potential for false positives (*i.e.*, incorrectly attributing MP counts to the environment rather than contamination), thereby reducing the risk of overestimating environmental MP pollution.

Within this context, the use of disposable laboratory gloves has been questioned in the recent QA/QC literature. While glove use is occasionally necessary to protect researchers from harsh reagents in MP sample processing, glove use is primarily suggested as a measure to protect environmental MP samples.[29–33] Yet, laboratory gloves have been shown to release non-volatile residues since the early 2000s.[34–37] Surprisingly, this finding had not been reported in the MP literature until 2020, when Witzig *et al.* reported that laboratory gloves submerged in water leached residues that were misidentified as polyethylene (PE) by μ-Fourier transform infrared (μ-FTIR) spectroscopy and μ-Raman spectroscopy.[38] The publication indicated that the residues, comprised of stearate salts used to release gloves from their moulds during manufacturing,[34] exhibit hydrocarbon structures similar to MPs like PE, and thus their vibrational spectra resemble one another.[38] While stearates are small

[a]*Department of Chemistry, University of Michigan, Ann Arbor, MI 48109-1055, USA. E-mail: ajmcneil@umich.edu*

[b]*Department of Statistics, University of Michigan, Ann Arbor, MI 48109-1107, USA*

[c]*Macromolecular Science and Engineering Program, University of Michigan, Ann Arbor, MI 48109-2102, USA*

[d]*Department of Electrical Engineering and Computer Science, University of Michigan, Ann Arbor, MI 48109-2122, USA*

[e]*Program in the Environment, University of Michigan, Ann Arbor, MI 48109-1041, USA*

molecules and MPs are polymeric, the critical difference between vibrational measurements of the identities is the presence of a carboxylate salt functional group in the stearate species that is absent from PE. Witzig *et al.* found that using μ-FTIR standard stearate reference libraries, where the unique carboxylate peak is visible, helped to reduce MP overestimations by automated spectral library matching.[38] However, traditional approaches to identify environmental spectra, such as reliance on topmost hit quality index (HQI), could not address Raman spectral similarity between stearates and PE because the distinguishing carboxylate vibrational mode is not Raman active. Along these lines, there is a lack of open-access stearate vibrational reference spectra to date, leaving a gap in the MP community's ability to identify contaminants from glove contact using the field's most common analytical techniques.

In this work, we show that dry surface contact with laboratory gloves also leads to an overestimation of MPs when vibrational micro-spectroscopy data is subjected to traditional library matching. First, we evaluate the QA/QC recommendations of recent MP reviews to understand current guidelines regarding glove use. Next, we quantify the release of stearates from seven common laboratory glove varieties under dry contact conditions *via* infrared and Raman analysis and illustrate that they are commonly misidentified using traditional, topmost HQI-based library searching approaches. To address the spectral and optical similarities between MPs and stearate species, we provide an open-access spectral library of stearate standards and outline methods to identify glove contamination in spectral datasets. After illustrating the application of our techniques to a contaminated environmental dataset, we provide recommendations on avoiding, recognizing, and salvaging vibrational spectral datasets impacted by glove contamination to aid the MP community to more accurately quantify environmental MP pollution.

Experimental

Instituting QA/QC protocols for sample handling

Laboratory gloves were not worn during sample handling related to quantifying stearate salt release. Researchers used soap and tap water to thoroughly wash their hands before handling all sample materials with metal tweezers. Samples for controlled, dry contact experiments were prepared in a laminar flow hood (Purair FLOW-36-A) purged with HEPA-filtered air while a cotton laboratory coat was worn. Samples were housed in capped single-stub microscopy storage tubes (Ted Pella, 16630) while not in use to protect from atmospheric MP deposition. Analysis was conducted in the closed instrument, and a cotton laboratory coat was worn when the instrument was open to external air. Procedural blanks were prepared, collected, and analyzed alongside samples to assess contamination not originating from laboratory gloves.

Investigating dry residue release from laboratory gloves

Aluminum-coated silicon substrates (Angstrom Engineering, QA05-00491, 4-inch diameter, 100 nm thick coating, average size 5 mm × 6 mm) were prepared in the same purged laminar flow hood. Seven types of chemically rated disposable laboratory gloves were selected for testing. We tested three latex (L) and three nitrile (N) gloves, as well as one nitrile cleanroom (CR) glove (see SI Section SII). These choices reflect the QA/QC literature reports of the most often suggested glove materials. We hypothesized that the strict contaminant-free standards of cleanrooms would necessitate particulate-free gloves, and a cleanroom glove was thus investigated as a potential alternative to gloves with manufacturing processes that include stearates. The finger portion of each unused glove was cut with scissors, and a glass microscope slide was inserted into the newly opened fingertip portion of the glove and secured with tape (see SI Section SIII). To reduce the potential of depositing MPs from cutting the glove onto the surface for analysis, the glove was cut ~50 mm from the region of contact. This process was repeated with a new glove for each sample type, generating two slides with unique gloves from the same box.

Using a TA × XT-Plus texture analyzer, each substrate was brought into contact with a glove-covered microscope slide at a constant speed (Fig. 1). The substrate exerted a contact force of 30 N to the glove-covered microscope slide prior to retraction (see SI Section SIII). A 30 N contact force (equivalent to the strength required to lift ~3 kg on Earth) was selected to mimic contact between a gloved hand and a laboratory surface or sample and to maintain consistency between trials of different gloves. This force corresponds to the average maximum force that an index finger can exert on a plate resting under the finger.[39] Notably, this force does not exceed the average pinch strengths (3–5 kg)[40,41] and grip strengths (>25 kg) of humans.[42] As Witzig *et al.* evidenced that stearate salts persist in submerged aqueous conditions and can be transferred to a sample surface *via* filtration, the chosen force is representative of a researcher's manipulation of materials in the laboratory such as filtration units,[38] digestion or density separation glassware, or the sample itself in the laboratory.

This process of controlled contact was repeated with a second aluminum-coated silicon substrate and second glove, generating two substrates from two unique gloves. Two procedural blanks (aluminum-coated silicon pieces that were prepared, transported, and handled in the same manner as the samples but did not contact a glove surface), were used to assess external contamination in the workflow (SI Section SXI). This yielded eight sets of replicate substrates.

To collect simultaneous infrared and Raman spectra of glove residues imprinted on the aluminum-coated silicon substrate, a mIRage optical photothermal infrared (O-PTIR) + Raman microscope (Photothermal Spectroscopy Corp.) equipped with computer-controlled capabilities was used (see SI Section SIII). Briefly, the mIRage system collects simultaneous photothermal infrared (PTIR) and Raman spectra *via* a pulsed infrared quantum cascade laser and a 532 nm continuous wave probe laser. The PTIR (10 averaged scans, 2 cm^{-1} resolution, from 948–1860 and 2698–3002 cm^{-1}) and Raman (3 × 30 s average scans, 30 s delay, 3.4 cm^{-1} resolution, from 170–4000 cm^{-1}) spectra were collected with 48% infrared power and 5% probe power (see SI Section SIII). Previous studies have validated this

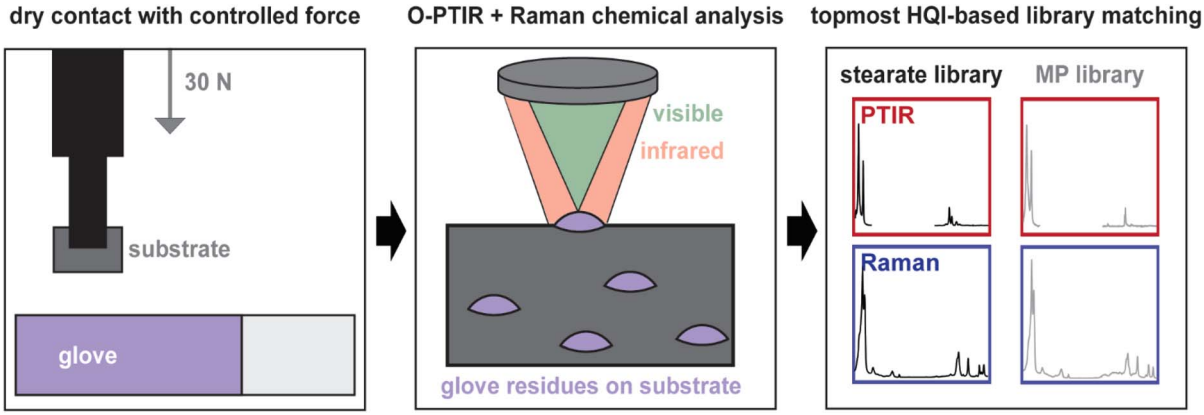

Fig. 1 Schematic workflow depiction of glove residue collection with 30 newton (N) applied force, chemical analysis *via* optical photothermal infrared (O-PTIR) + Raman spectroscopy, and stearate (black) or microplastic (MP, grey) spectral library matching using photothermal infrared (PTIR) or Raman spectra.

method for identifying MPs down to <1 μm in size.[43] As it was not possible to analyze all particles on the substrate surface, we adopted a subsampling strategy that targeted three random locations for chemical analysis on each substrate. The goal of this strategy was to obtain ~100 photothermal infrared PTIR and Raman spectra from residues >0.5 μm in projected area diameter from each substrate. Randomly generated coordinates were used to collect chemical and optical information, and the featurefindIR® (PTIR Studios v4.6) was used to tabulate particle location and projected area diameter based on image contrast (see SI Section SIII). On average, this collection led to random chemical canvassing of 5% of the substrate area and comprised ~200 PTIR and Raman spectra per glove variety across two replicate samples in six unique locations. To increase representative sampling efforts for particle size information,[44] the random optical imaging canvased an average 16% of each substrate area.

PTIR and Raman spectra were preprocessed prior to library matching, leading to the exclusion of low signal-to-noise ratio (SNR) PTIR spectra, where signal could not be distinguished from noise, and saturated Raman spectra (see SI Section SV). The remaining PTIR and Raman residue spectra were matched to an in-house reference library spectra comprised of stearate standards with different metal cations (calcium, magnesium, sodium, and zinc) and three common MP identities (high-density polyethylene (HDPE), polypropylene, and polystyrene, see SI Section SIV). Pearson correlation coefficient (PCC) was used to calculate HQI, where the reference spectrum identity with topmost HQI over a threshold of 0.7 (on a range of 0 to 1) was accepted as the residue spectrum identity, mimicking traditional library matching methods.[45–47] It should be noted that, by spectral matching, stearates were the dominant identity of particles transferred from most glove surfaces, yet other identities (in addition to HDPE, PS, and PP) were also present (Fig. S38 and S39).

As conventional FTIR microscopes are limited by a spatial resolution of ~10 μm,[48–50] but the average particle projected area diameter in this study was 1.6 ± 0.8 μm (Fig. S46), we wanted to investigate if the agglomeration of these particles would influence FTIR measurements. For this purpose, a gloved (L1) hand contacted an unused aluminum-oxide filter, which is extensively used for single-particle micro-spectroscopy measurements in the MP literature.[51–53] Stearate contamination was evidenced by Nicolet iN10 Infrared Microscope (Thermo Scientific) transmission measurements (see SI Section SVII). In brief, the cooled detector with 15 μm × 15 μm apertures were used to collect signal (1350–4000 cm^{-1}, 32 scans, 4 cm^{-1} resolution) of residues present on the filter surface. Guidance and results from applying the workflow established herein to μ-FTIR spectra, rather than PTIR spectra, is also presented (SI Section SVII).

Conformal prediction

Conformal prediction (CP) is a statistical method that guarantees a user-defined theoretical confidence in a set of predictions.[54,55] This method is described in detail in the work of Clough and Ochoa Rivera *et al.*[46] In brief, CP uses a calibration set of identified spectral data to create a distribution of HQI when matching to a reference library (see SI Section SVIII). The HQI can be calculated using any chosen similarity metric, such as PCC or nearest neighbor (NN).[46] The user-defined theoretical confidence guarantee (*e.g.*, 95%) describes a proportion of the HQI distribution, effectively creating a new, data-driven HQI threshold that will be used to evaluate predicted spectral identities. Next, a test set of unidentified spectra is matched to the reference library. If the HQI meets or exceeds the threshold described by the theoretical confidence guarantee, the identity is added to the prediction set. The user then has the same theoretical confidence guarantee that the prediction set includes the true spectral identity of the unidentified spectrum. This guarantee hinges on the assumption that the HQI distribution of the calibration spectra is exchangeable with that of the unidentified, test spectra (see SI Section SVIII). Fortunately, the CP framework only serves to quantify uncertainty in the prediction, meaning that only the performance of the similarity metric is influenced by spectral quality. Herein, we applied CP using NN similarity metric with a 95% theoretical

confidence guarantee to the Raman spectra of glove residues (see SI Section SVIII).

Application to glove-contaminated environmental dataset

To illustrate dataset recovery, a mIRage O-PTIR + Raman vibrational dataset containing 2653 spectra from passive atmospheric particle collection in four Michigan locations in the spring of 2023 was used (see SI Section SIX). This dataset, collected according to MP literature QA/QC recommendations, presents a case study to differentiate stearates and environmental MPs, as aluminum-coated silicon substrates were prepared within a laminar flow hood with nitrile gloves (type N3), and the substrates were then deployed for month-long periods in the environment to collect MPs dry depositing from the atmosphere (see SI Section SIX). To illustrate the recovery of each signal, we followed the same preprocessing pipeline outlined herein and used the mIRage MP library to catalogue PTIR and Raman matches (HQI $\geq$ 0.7) to HDPE. This approach gave 38 PTIR matches and 110 Raman matches that would have been identified as polyethylene when following a traditional library matching routines.[45–47] All spectra were manually evaluated for predicted identities of "stearate", "HDPE", and "uncertain", where "uncertain" was assigned in cases where low spectral fingerprint SNR or Raman fluorescence impeded manual prediction, or in cases where the spectrum did not appear to be either identity (see SI Section SIX). Spectra that were manually assigned an "uncertain" identity were excluded from automated predictions, as additional data would be required for an analyst to manually assign an identity to each spectrum. Separately, without consulting the manually predicted identities, the topmost HQI of the extended fingerprint region (980–1800 cm^{-1}) of the remaining 19 PTIR matches were calculated with respect to the mIRage MP and stearate libraries. Similarly, CP, with the NN similarity metric and a 95% theoretical confidence guarantee, was used to predict the identities of the remaining 21 Raman HDPE matches (here used as a new test dataset) using the same calibration set and theoretical confidence guarantee previously employed.

The instrumentation and preprocessing workflow used herein provided a strong framework for understanding how to best differentiate stearate glove contaminants from environmental MPs. However, as the procedures and instrumentation in this study may be impractical for routine applications of the workflow, we also provide a simplified user guide on method application and interpretability (see SI Section SX).

Results and discussion

Current glove use recommendations

After surveying the MP literature, we identified a total of 26 review articles (published 2018–2024) that included advice on glove use as a QA/QC measure. Glove use was recommended by 81% of articles (Fig. 2). Notably, only two reviews mentioned that contact with the sample should be limited. When comparing reviews published before and after the Witzig *et al.* findings that MP false positives arise from wet contact with gloves (September 2020), there was only a modest 7% decrease in articles that suggested gloves be worn to protect samples (Fig. S1). In addition, there lacks a consensus on the best glove material for MP research (Fig. 2). Latex gloves were the major material (38%) recommended by reviews, and an increase in latex recommendations was observed following the Witzig *et al.* publication (Fig. S2). This shift is surprising, as Witzig *et al.* showed similar rates of MP false positives from both materials, and the rationale for latex gloves over other materials is absent.[38] Overall, there remains division among QA/QC recommendations to the MP community regarding glove use, and our results on glove-based contamination causing MP false positives *via* dry contact should enhance evidence-based decision-making on MP sample protection measures.

Spectral identification of glove residues

Stearate salts are used as mold-release agents in glove manufacturing,[34,38] but may cause MP false positives by vibrational micro-spectroscopy. To evaluate if dry contact with laboratory gloves deposits stearates to a surface and if those stearates lead to MP false positives when standard stearate libraries are not used, the seven selected disposable laboratory gloves (representing nitrile, latex, and nitrile cleanroom materials) were brought into controlled contact (30 N) with an aluminum-coated silicon substrate, then chemically analyzed

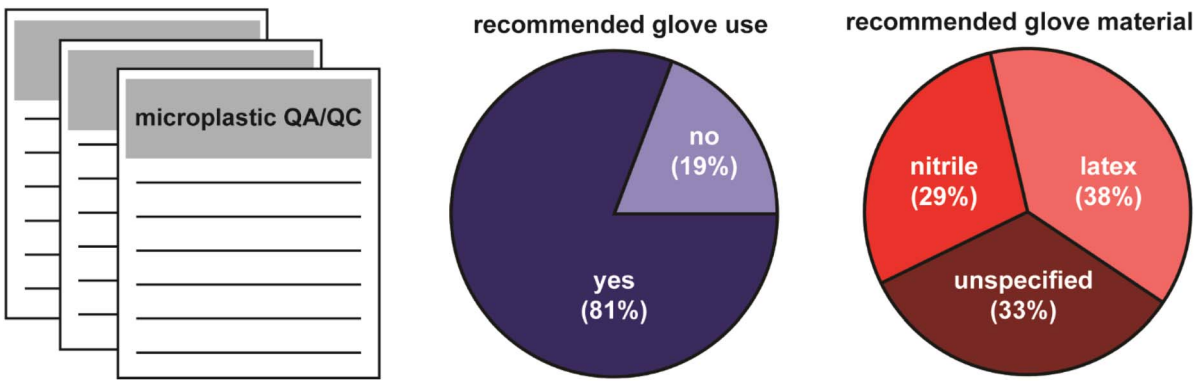

Fig. 2 Results of microplastic quality assurance and quality control (QA/QC) review article literature search in terms of recommended glove use ($N = 26$) and recommended glove material ($N = 21$).

with O-PTIR + Raman spectroscopy. Individual collected spectra of glove residues were preprocessed and subjected to automated library searches with both in-house MP and stearate reference libraries. When following a traditional matching approach to spectral identification using the topmost returned HQI as the unknown spectrum's identity and exclusively comparing to MP reference spectra, nearly all the tested gloves were found to cause MP false positives, with HDPE being the dominant MP identity recorded (Fig. S37). The number of false positives varied significantly between samples, with the most prolific glove, L1, releasing >7000 residues per mm^2 area that were mistakenly identified as MPs when normalized to the area analyzed per substrate and corrected to account for blank contamination (see SI Section SXI). Glove-to-glove variability and contact point topology likely influence the high standard deviation between samples, giving a mean quantity of 2100 $\pm$ 2400 false positives per mm^2 and 1800 $\pm$ 2400 false positives per mm^2 for all gloves by PTIR and Raman, respectively (Fig. 3a). Although some variation can be seen between the number of matches by PTIR and Raman signals, this discrepancy may be explained by the differing proportions of spectra excluded in the separate preprocessing pipelines (Fig. S11 and S13). This finding illustrates that, when using the most common matching methodologies in the MP literature (accepting topmost matching MP identity above a 0.7 HQI threshold), common laboratory glove use will likely cause overestimation of MP quantities through dry, physical contact with laboratory materials.

When stearate reference libraries are used in place of MP libraries, calcium stearate was the major predicted identity (Fig. S36). As seen in Fig. 3b, the number of misidentified MPs per sample translates almost directly to the number of stearates released per unit area. While all gloves released non-volatile residues as evidenced from optical image data (Fig. S36), both CR and L3 samples release far fewer stearates, and thus generate fewer false positives per unit area than other glove varieties. While the CR gloves are advertised to feature low particulate levels suitable for the ultrapure cleanroom environment,[56] the explanation for why L3 releases so few stearates is unknown, as the company indicated *via* personal communication[57] that calcium stearate use was common with their disposable latex glove manufacturing. Although using procedural blanks alongside our provided stearate vibrational spectra reference libraries may reduce MP false positives,[51,58,59] stearate contamination will unevenly impact samples due to glove-to-glove variability and differences in applied pressure. Researchers can expect stearate salts to be present on the surface of common latex and nitrile laboratory gloves that encounter laboratory materials, exposing an environmental sample to potential MP false positives. Therefore, the best practice to reduce stearate contamination and the potential for overestimation of MPs in environmental samples is to avoid glove use. However, if harsh reagents are necessary, researchers should not hesitate to use gloves for personal protection; they should opt for a glove that addresses occupational safety needs

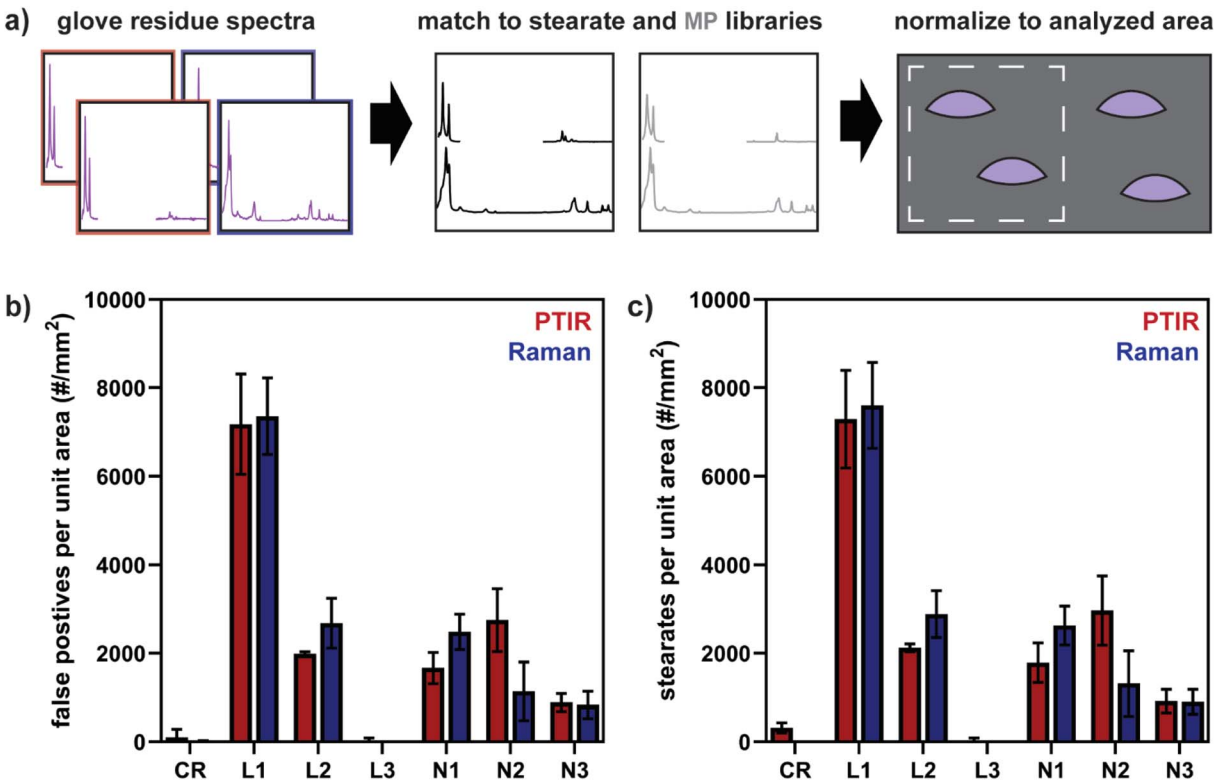

Fig. 3 Library matching (a) workflow including matching unknown residue spectra to color-coded stearate (black) and microplastic (MP, grey) reference spectra, normalizing results to analyzed area, and results of PTIR and Raman (b) MP (*i.e.*, false positive) and (c) stearate spectral matches per unit area for each glove, where error bars refer to the standard deviation between two replicate samples. CR refers to cleanroom, L to latex, and N to nitrile glove materials. Samples with the same numeric abbreviation (*e.g.*, L1 and N1) were sourced from the same manufacturer.

while maintaining a low non-volatile residue release rate, such as a cleanroom glove alternative.

Optical analysis of glove residues

Not only are the PTIR and Raman spectra similar between stearate contaminants and microplastics, the physical characteristics and morphology appear alike as well. Optical and electron micrographs of glove residue (L1) and post-consumer HDPE were collected (see SI Section SVI). A similar gradient in contrast is observed *via* optical images from the mIRage system for particles identified as HDPE and stearates (Fig. 4). *Via* tilt-SEM, both non-volatile residues from glove contact and HDPE are visualized to be ridged, thin particles that illustrate a film-like morphology. The lack of distinguishing features highlights that identification based on optical or morphological features is not possible. Size characteristics collected from the dry, glove residues indicate a mean particle projected area diameter of 1.6 ± 0.8 μm (Fig. S47) and MPs in the lower size class (<10 μm) are extremely relevant to environmental transmission and critical health impacts.[60–62] With dry release of stearates from laboratory gloves therefore disproportionately overestimating MPs in this crucial, small size class, a method capable of routinely distinguishing between plastic and glove contaminant identities is required.

Modified spectral regions to identify contaminated infrared datasets

While it was expected for stearate spectra to be indistinguishable from HDPE *via* Raman library searching due to the Raman-inactive carboxylate vibration, a surprising result in our study was the inability of traditional HQI approaches to distinguish infrared spectra, where the carboxylate stretch (1550–1580 cm^{-1}) of the stearate spectra is absent from HDPE spectra.[38] When unidentified residue spectra are searched, automated library matching algorithms produce high HQI scores to reference spectra of both stearates and MPs, despite the distinguishing stearate spectral feature (Fig. 5). Indeed, the mean difference between topmost HQI scores ≥0.7 to stearate and MP identities is only 0.01 for the PTIR data (Fig. S41). When both the stearate and MP libraries are used as reference libraries for the PTIR spectra, 66% of glove-based particle spectra matched with higher HQI to stearate spectra than HDPE spectra (Fig. S38). Contrarily, in the Witzig *et al.* publication, nearly 90% of the infrared spectra were assigned stearate identities by topmost HQI.[38] The difference in distinguishing power is likely due to particle size. In our work, the vast majority of residues are <2 μm in projected area diameter (Fig. S47), whereas in the Witzig *et al.* study, 82% of particles released from gloves soaking in water were between 5 and 20 μm.[38] The smaller particle size leads to a lower SNR, causing the spectral identification method to struggle with distinguishing noise from recorded intensities.[45,47,50,63–65] Additionally, use of single-particle PTIR reference libraries *versus* bulk plastic measurements from a μ-FTIR system influences matching results, as traditional, topmost HQI-based spectral matching methods are subject to influences beyond just changes in signal intensity and peak position (*e.g.*, instrument collection parameters, particle size, and SNR),[47,50,63–67] indicating wholly different spectral matches depending on the conditions employed (see SI Section SXII). Combined, these studies indicate that stearates are released from laboratory gloves under wet and dry conditions, and their small size presents unique challenges in distinguishing their identity from environmental MPs *via* vibrational micro-spectroscopy.

Despite the distinguishing carboxylate vibration, traditional HQI-based approaches struggle to differentiate stearate and HDPE PTIR spectra. In addition, because variable glove contact conditions preclude the use of a procedural blank correction as a method to account for stearate contamination, more sophisticated spectral methods are required to distinguish MPs from contaminants. Specifically, one proposed solution to the challenge of spectral noise influencing similarity measurements is restricting library searches to specific ranges of wavenumbers where significant differences in vibrational peaks occur. This method reduces the influence of regions with high spectral similarity (*e.g.*, peak shape or intensity) from outweighing other factors of resemblance, such as peak position, and limits the influence of noise falsely inflating HQI scores.[68] This approach has been previously used to decrease the influence of environmental weathering and spectral noise on automated spectral searching methods,[67,69,70] and to increase compatibility between unidentified spectra and reference spectra collected on different instruments.[64,68,70] When applying narrower spectral ranges to the glove residue PTIR spectra, a distinction by topmost HQI score was only possible between the two species when the extended fingerprint (980–1800 cm^{-1}) region was

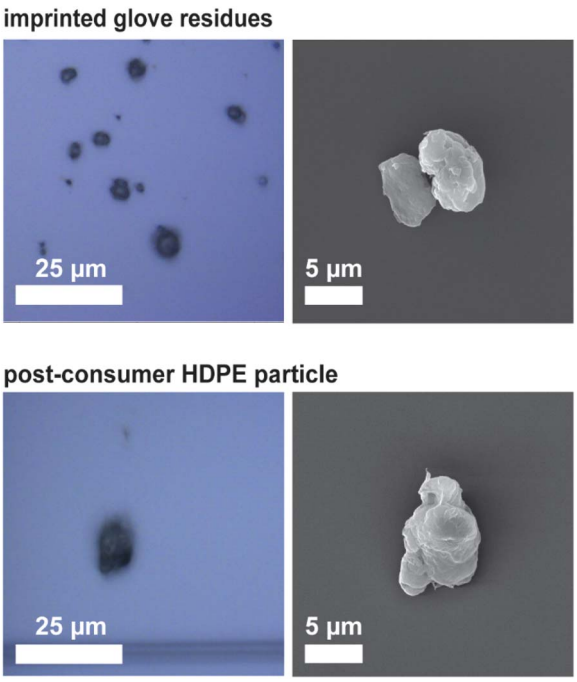

Fig. 4 Visually indistinguishable images of imprinted glove residues and post-consumer high-density polyethylene (HDPE) particle *via* mIRage 40× optical objective (left) and scanning-electron microscopy at 45° tilt (right).

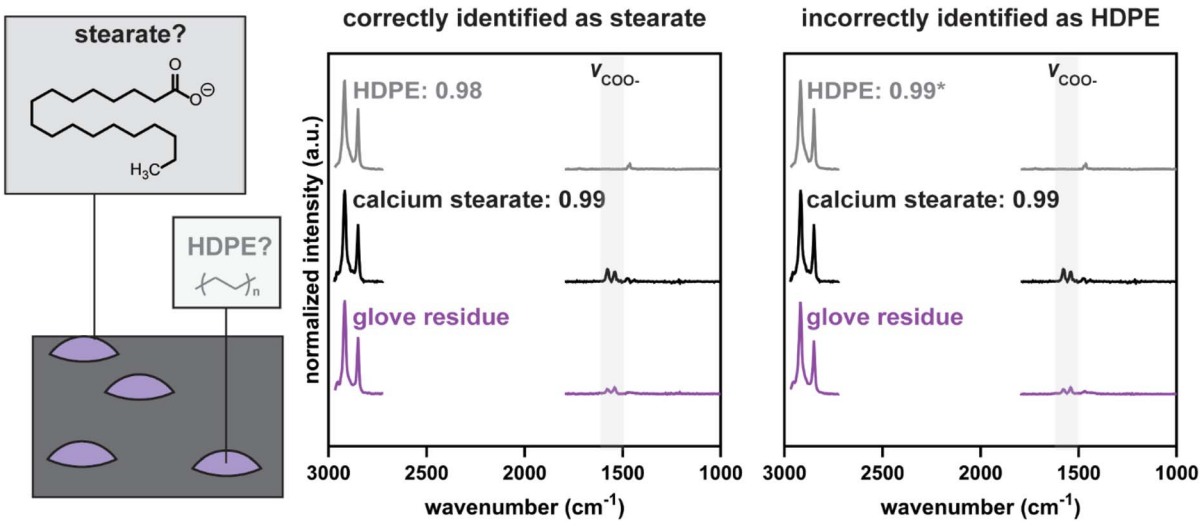

Fig. 5 PTIR spectra of stearate glove residue alongside reference spectral matches with topmost hit quality index (HQI) for spectra identified as calcium stearate and high-density polyethylene (HDPE) by traditional library matching methods. The distinguishing carboxylate stretch region of the spectrum is highlighted, and the asterisk indicates a higher HQI by less than 0.01.

searched (Fig. 6). This finding shows that the high degree of similarity in the C–H stretch region (2720–2980 cm^{-1}) leads to overestimation of MPs when traditional HQI-based matching approaches are used without modification. As the spectral fingerprint region is not reliable for all topmost-based HQI traditional library searches,[66] infrared datasets that are suspected to be glove-contaminated should first be traditionally library matched with a MP reference library to differentiate organic species (*e.g.*, stearates and polymers) from inorganic matter. Following this, the unidentified spectra that match (HQI $\geq$ 0.7) to MP references should then be truncated to the extended fingerprint range (where the most vital distinguishing peaks are present for organic species that exhibit similar C–H stretch regions) and compared to references of both stearates and MPs. Visual inspection should then be used to evaluate the quality of automated predictions. Visual inspection is specifically important for weathered MPs, which may exhibit higher carbonyl indexes than pristine polymers.[71] Fortunately, the location of the carbonyl peak of weathered PE (*i.e.*, 1680–1800 cm^{-1}) is outside the carbonyl peak range observed of stearate reference materials and glove-imprinted particles (*i.e.*, 1550–1580 cm^{-1}),[36,72–74] and both automated differentiation (see SI Section SVII) and visual confirmation of automated matches will reduce false positives. Using modified spectral ranges and the stearate spectral references supplied herein, traditional library searching methods can thus be tweaked to address glove-based contamination compounded by SNR impacts of particles in these most critical MP size ranges.

Conformal prediction to identify contaminated Raman datasets

Although previously reported to be "impossible to distinguish" due to inactive carboxylate vibrations,[38] higher acquisition times led to differentiable peaks being resolved in the Raman spectra of HDPE and calcium stearate (see SI Section SXIII for peak assignment). As seen in Fig. 7, when the spectral region of 1000–1600 cm^{-1} is further evaluated, a distinct stearate peak relating to skeletal C–C stretching and C–C–C bending is visible at 1106 cm^{-1} and is absent from the HDPE spectrum.[75,76] This peak is visible in all the stearate Raman reference spectra, despite lower SNR due to fewer averaged integrations (see SI Section SIV). Additionally, a C–H bending peak (relating to chain packing) at 1416 cm^{-1} is visible in the HDPE spectrum that is lacking in the calcium stearate spectrum.[77] While this peak may also be used as a tool to differentiate μ-Raman spectra of PE and stearates, the appearance of this peak is dependent upon the crystallinity of the analyzed polymer.[78] For pristine HDPE and low-density PE (LDPE), distinction with this peak is feasible due to the crystalline packing domains of the polymer; however, linear low-density PE (LLDPE) spectra lack this crystalline peak due to frequent chain branches, making it more challenging to distinguish contamination from LLDPE than from other PE types.[79,80]

The small differences between stearate and HDPE reference Raman spectra necessitate a more sophisticated method than traditional library matching. While a recent effort improved on HQI-based distinguishing of PE from stearic acid with machine-learning methods,[65] this method was not extended to the salts common in glove manufacturing and lacks uncertainty quantification on the single-spectrum level. To fill this need, CP was employed to return prediction sets of possible chemical identities for unidentified spectra that show similarity to multiple reference spectra. Both Pearson correlation coefficient and nearest neighbor similarity metrics were used with CP to compare the performance of absolute and relative metrics with the same 95% theoretical confidence guarantee (see SI Section SVIII). In brief, relative metrics like NN reduce the number of matches with high HQI scores, thereby reducing manual analysis of predicted identities to make NN more efficient than PCC (Fig. S24). When the glove residue spectra were used with CP,

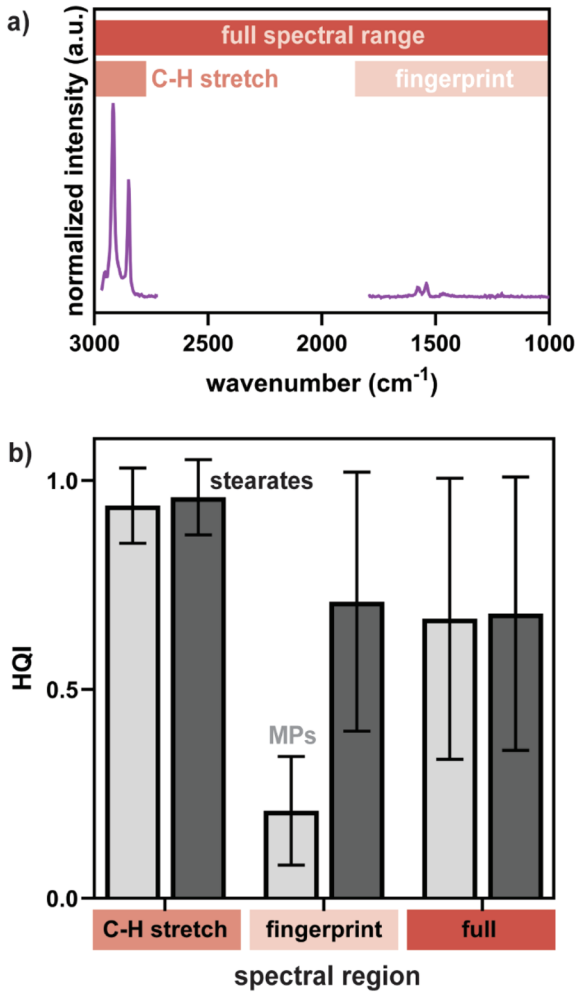

Fig. 6 Depiction of (a) PTIR spectra of stearate glove residue with highlighted spectral ranges and (b) mean HQI of each spectral region when matched to stearate (dark grey) and microplastic (MP, light grey) reference spectra. Error bars refer to the standard deviation between HQI scores.

most prediction sets included both stearate and MP identities (Fig. 8). However, as opposed to PCC, which assigned all glove-based spectra both MP and stearate prediction identities, NN assigned nearly half with only stearate predictions. As a relative metric, it is likely that NN is picking up on small differences between the residue spectrum and the reference examples, such as those indicated in Fig. 7, to better distinguish between MP and stearate identities. Use of a more efficient metric like NN indicates that stearate contamination is present in the Raman dataset and reduces MP false positives due to blanket acceptance of reference identity with the topmost HQI score.

For cases of high similarity between spectral identities, CP indicates when manual inspection is necessary to achieve statistical confidence in particle identity by returning multiple identities with close HQI scores. Raman datasets with suspected glove contamination should therefore undergo analysis with CP using the NN metric. As CP returns prediction sets on the single-spectrum level and HQI is suggestive of identity rather than prescriptive, prediction sets with both stearate and MP identities present should be manually identified to recover the dataset. The analyst may be able to discern the distinct Raman peaks between identities (depending on the spectral resolution), or may opt to collect additional information (*e.g.*, infrared or thermal data) to confirm the particle's identity. In this way, CP identifies contaminated datasets and outlines the manual assessment necessary to salvage the dataset at the individual spectrum level. Conformal prediction can also be used with additional classifiers, such as the machine-learning approach put forth by Lim *et al.*,[65] which exhibited high accuracy for fatty acid *versus* PE classifications. Because CP is an uncertainty framework that wraps around any metric, one can use any classifier for spectral labeling and can compare metric performance using the prediction set size and empirical confidence.[46] Microplastic researchers can adopt the CP workflow to recover contaminated datasets by using the open-access code and user-guide provided in the work of Clough and Ochoa Rivera *et al.* in conjunction with the open-access stearate libraries provided herein.[46]

Application to glove-contaminated environmental dataset

To establish that the solutions put forth herein are suitable to use with contaminated environmental datasets, we turned to a collection of mIRage O-PTIR + Raman vibrational spectral data previously acquired with the goal of quantifying atmospheric microplastics in four Michigan locations (see SI Section SIX).

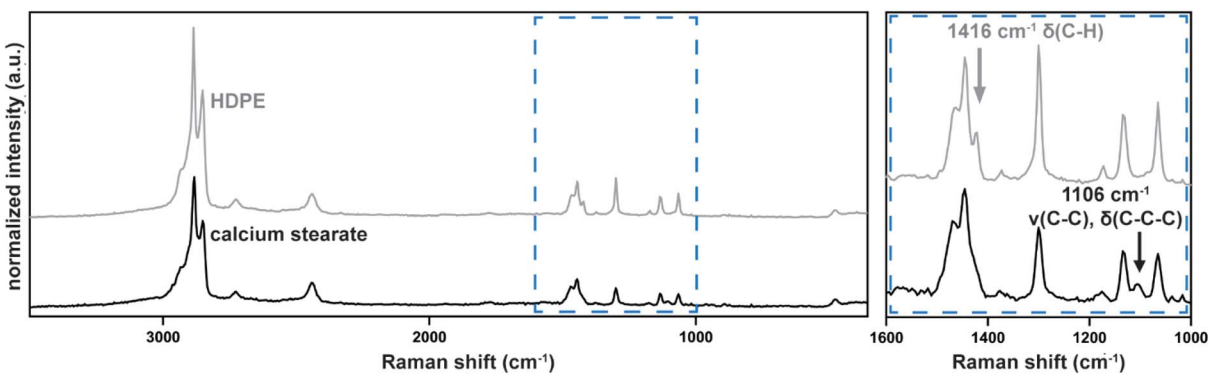

Fig. 7 Raman spectra of high-density polyethylene (HDPE) compared to calcium stearate, distinguishable *via* spectral features highlighted in the blue, dashed region of the plot.

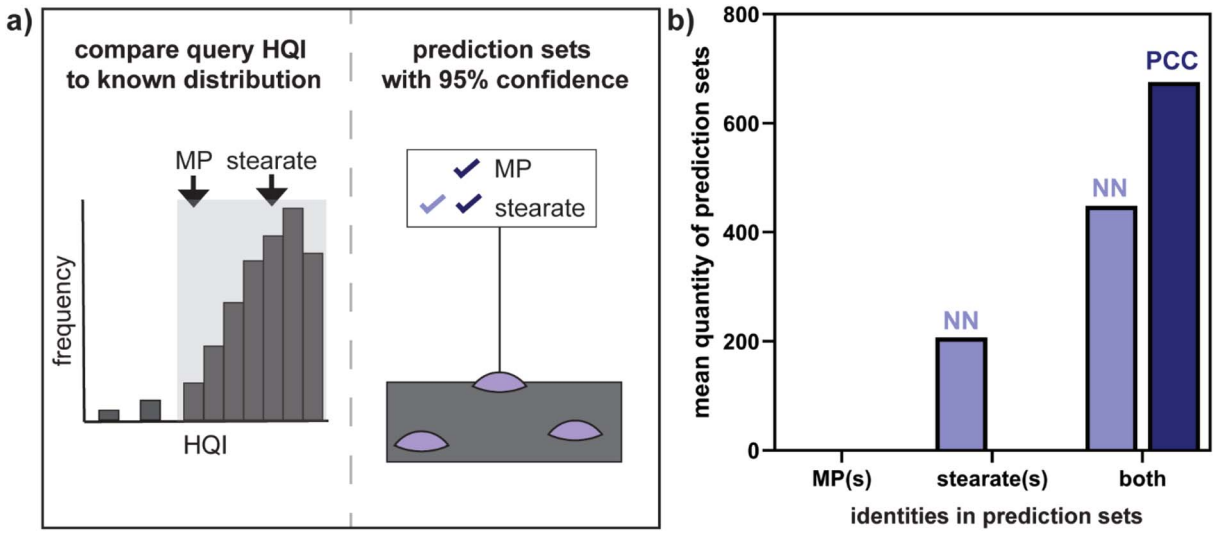

Fig. 8 Conformal prediction (a) schematic overview, where microplastic (MP) and stearate identities are compared to the 95% confidence interval (shaded) on a known distribution of hit quality index (HQI) to generate prediction sets for each similarity metric, and (b) mean quantity of prediction sets including MP identities, stearate identities, or both MP and stearate identities for nearest neighbor (NN) and Pearson correlation coefficient (PCC).

Following literature recommendations, we wore nitrile gloves (specifically, type N3). We used a laminar flow hood to prepare aluminum-coated silicon substrates, as in the Methods section herein, for passive atmospheric particle deposition. Chemical analysis following the sampling campaign's collection periods (see SI Section SIX) identified PE spectral library matches on procedural blanks and revealed MP quantities far greater than previously reported. Careful analysis of this dataset led to our discovery of dry-contact transfer of stearates from gloves that falsely inflated MP quantities *via* vibrational spectral matching. While we could not use the dataset for its intended purpose, it demonstrates how real-world samples can be impacted by glove-based contamination even when standard MP protocols are used. Using this data, we present a case study for the application of our solutions to glove-contaminated environmental datasets with small (<10 μm) MPs, where spectral data quality can impede quantification efforts at this most critical size class.

Following a traditional matching approach, we first used the mIRage MP library to identify HDPE matches (PCC, HQI $\geq$ 0.7) for each preprocessed signal. Next, an analyst manually assigned identities of "stearate" or "HDPE" for all spectra where distinction was possible (see SI Section SIX). Treating each signal separately, we then compared the automated predictions from our proposed recovery workflows (*i.e.*, extended fingerprint-based PCC HQI comparison for PTIR spectra and CP with NN and a 95% theoretical confidence guarantee for Raman spectra) to the analyst's predictions. As evidenced in Fig. 9a, the modified regions of spectral comparison successfully identified all 14 stearate examples in the PTIR environmental dataset. However, the automated prediction for PTIR HDPE spectra agreed with the analyst assignment for only three of the five spectra, indicating that the method may better indicate contaminant presence (*i.e.*, false positives) than HDPE presence (*i.e.*, true positives) in the sample. We hypothesize that the mismatch in PTIR automated prediction performance between identities is due to noise or aging artefacts in the HDPE spectra being mistaken as carboxylate vibrations by the similarity metric (Fig. S28). In our suggested workflow, visual confirmation of the automated results is expected to reduce the occurrence of HDPE false negatives. With the Raman environmental dataset, the 95% theoretical confidence guarantee CP prediction agreed with the analyst prediction for five HDPE spectra (Fig. 9b). For the other 16 spectra, the prediction set contained both HDPE and stearate identities, indicating that additional data may be required to differentiate the identities within the prediction set. To obtain this result, in which the automated prediction is more cautious than the trained analyst to identify environmental MPs, is valuable when identifying false positives in the smallest MP size ranges, where spectral quality diminishes as health and environmental impact surges. As in our workflow, CP prompts the analyst to review the spectrum for distinguishing peaks between predicted identities, and/or collect additional data to support the identification.

While we separately processed the PTIR and Raman spectra belonging to the environmental particles to highlight the applicability of the recovery workflows to independent infrared and Raman datasets, access to both the PTIR and Raman predictions for ten particles gave additional insight into the performance of the distinction methods with environmental data. Of the ten examples, there were three instances where the manual and automated predictions for PTIR and Raman disagreed. These three particles were predicted to be stearate contaminants based on PTIR spectra, yet were identified as HDPE based on Raman spectra. Upon inspection, the PTIR predictions were manually validated over the Raman predictions, which may have been incorrect due to reduced spectral quality compared to lab-generated Raman data and/or environmental aging, which can disrupt molecular crystallinity and reduce the intensity of distinguishing spectral peaks (Fig. S32).[81,82]

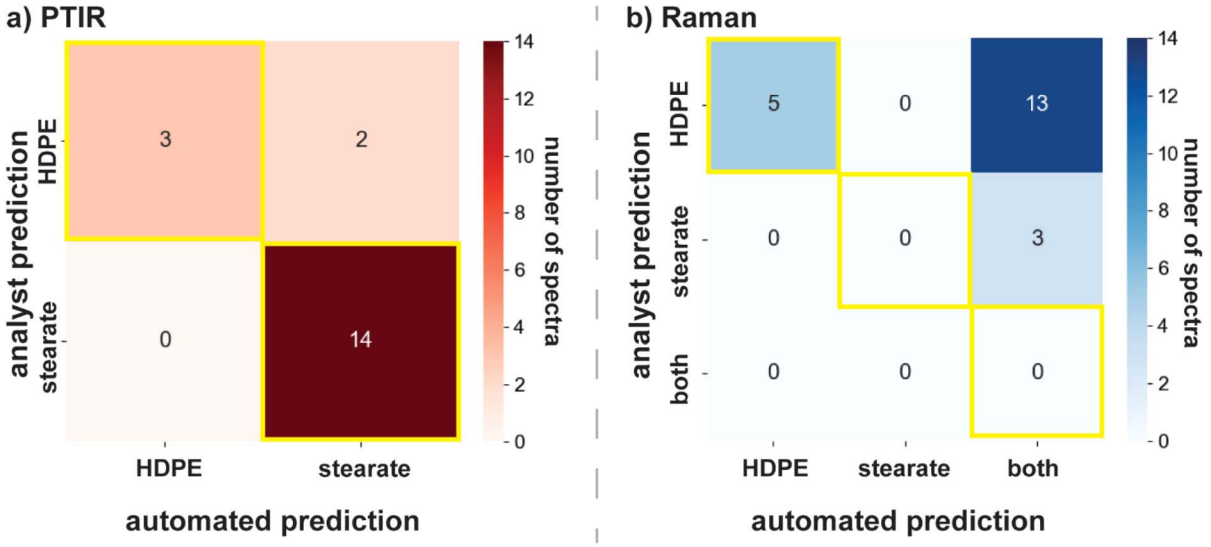

Fig. 9 Heat map representing (a) the number of PTIR spectra and (b) the number of Raman spectra of each identity predicted by the analyst (*y*-axis) and by the proposed automated solution (*x*-axis). Cells outlined in yellow along the left-to-right diagonal indicate spectra for which the analyst and automated prediction agree. For the Raman data, a predicted identity of "both" indicates that both HDPE and stearate identities were included in the CP prediction set.

To formally investigate the role of Raman data quality in the recovery workflow, we randomly selected a small number (≤5) of HDPE and stearate Raman spectra from the mIRage reference library and, using the same CP conditions as employed with the environmental data, repeated the random selection of spectra and generation of prediction sets 500 times (see SI Section SIX). Understanding the true identity of each spectrum allowed us to calculate both the mean prediction set size (*i.e.*, the number of predicted identities) and the mean empirical confidence (*i.e.*, the proportion of instances where the true identity is in the prediction set) for each reference identity. With this dataset, which exhibited notably higher spectral quality than the environmental dataset, CP achieved empirical confidence of greater than 93% for all identities, with a mean prediction set size of less than two identities (Fig. S33). This finding highlights the significance of data quality in predicting spectral identity, particularly when applied to environmentally aged particles. For Raman spectra, where distinction between stearate and HDPE identities is particularly challenging, high spectral data quality, especially where distinguishing peaks may be present (*i.e.*, 1416 and 1106 cm^{-1}) is essential (see SI Section SIX). When working to recover stearate-contaminated environmental MP datasets from the most analytically challenging MP size range, techniques that provide complementary identification data, such as O-PTIR + Raman,[43] and analysis routines that involve uncertainty quantification, like CP,[46] are pivotal to reduce MP false positives and better estimate environmental MP quantities.

Conclusions

In this work, we illustrated that dry contact with nearly all tested laboratory gloves impart stearate residues to a touched surface that lead to overestimating environmental microplastic quantities when using traditional topmost hit quality index-based approaches to spectral identification. Departing from previous studies, which indicated that stearates can be distinguished by infrared spectroscopy, our study indicates that the smaller size of stearates imparted by dry contact (<2 μm) cannot be distinguished from infrared nor Raman microplastic reference spectra with traditional library matching methods due to lower signal-to-noise ratios. We recommend that future microplastic quantification campaigns avoid glove use entirely, when possible, or employ gloves with low particle release rates. When glove use is unavoidable due to the need for personal protection, distinguishing between microplastic and contaminant species will require a data analysis routine (*i.e.*, modified spectral matching ranges and/or conformal prediction) more apt for this task than routine acceptance of a reference identity with topmost hit quality index.

To address the potential for overestimation of microplastic environmental quantities due to laboratory glove use with traditional spectral matching methods, we demonstrated that data analysis routines specific to the technique of spectral collection can address the high spectral similarity between stearate species and microplastic identities. We also evidenced the recovery of glove-contaminated environmental data, wherein the proposed methods successfully reduced MP false positives and provided insight into how data quality dictates method performance. While this article focused on the abilities of automated methods to identify vibrational spectra, manual assessment of spectral similarity remains key to correctly predicting chemical identity. By providing open-access reference libraries of various stearate species and a framework for assessing contaminated infrared and Raman vibrational spectral datasets, we implore microplastic researchers to address glove-based contamination and avoid overestimating microplastic pollution in the environment.

Author contributions

The manuscript was written through contributions of all authors. M. E. C. was involved with conceptualization, methodology, validation, investigation, writing – original draft, writing – review & editing, and visualization. E. O. R. was involved with methodology, software, validation, formal analysis, and investigation. A. M. A. was involved with methodology, validation, and investigation. R. L. P. was involved with validation and resources. J. P. was involved with software. H. E. T. was involved with investigation. A. P. A. was involved with resources, supervision, and project administration. A. T. was involved with resources, supervision, and project administration. A. J. M. was involved with conceptualization, resources, visualization, writing – original draft, writing – reviewing & editing, supervision, project administration, and funding acquisition. All authors have given approval to the final version of the manuscript.

Conflicts of interest

There are no conflicts to declare.

Data availability

The data supporting this article have been included as part of the supplementary information (SI). Supplementary information: additional experimental details, materials, and methods; selected PTIR and Raman microplastic and stearate reference library spectra. See DOI: https://doi.org/10.1039/d5ay01801c.

Acknowledgements

The authors acknowledge funding from the College of Literature, Science, and Arts at the University of Michigan. R. L. P. was supported by an NSF Graduate Research Fellowship (NSF-GRFP) DGE-2241144. M. E. C. was partially supported by the University of Michigan Rackham Graduate School through a merit and predoctoral fellowship. The authors would like to acknowledge the professors and students of the Mapping, Measuring, and Modeling Microplastics in the Atmosphere of Michigan team for their support and helpful discussions. The authors thank Jennifer Connor, Curtis Refior, Amy Pashak, Megan Phillips, Josh Hubbard, Bill Joyce, and David Lee for their community partnership. The authors would also like to thank former Dean Anne Curzan from the College of Literature, Science, and the Arts at the University of Michigan for funding this work through the "Meet the Moment" grant program. The authors acknowledge technical support from the Michigan Center for Materials Characterization.

References

1 R. Geyer, J. R. Jambeck and K. Lavendar Law, *Sci. Adv.*, 2017, **3**, e1700782.
2 L. Van Cauwenberghe, A. Vanreusel, J. Mees and C. R. Janssen, *Environ. Pollut.*, 2013, **182**, 495–499.
3 A. Abel de Souza Machado, C. W. Lau, W. Kloas, J. Bergmann, J. B. Bachelier, E. Faltin, R. Becker, A. S. Görlich and M. C. Rillig, *Environ. Sci. Technol.*, 2019, **53**, 6044–6052.
4 Y. Deng, Y. Zhang, B. Lemos and H. Ren, *Sci. Rep.*, 2017, **7**, 46687.
5 K. Zhang, A. Hossein Hamidian, A. Tubić, Y. Zhang, J. K. H Fang, C. Wu and P. K. S. Lam, *Environ. Pollut.*, 2021, **274**, 116554.
6 N. B. Hartmann, T. Hüffer, R. C. Thompson, M. Hassellöv, A. Verschoor, A. E. Daugaard, S. Rist, T. Karlsson, N. Brennholt, M. Cole, M. P. Herrling, M. C. Hess, N. P. Ivleva, A. L. Lusher and M. Wagner, *Environ. Sci. Technol.*, 2019, **53**, 1039–1047.
7 J. P. G. L. Frias and R. Nash, *Mar. Pollut. Bull.*, 2019, **138**, 145–147.
8 J. R. Jambeck, R. Geyer, C. Wilcox, T. R. Siegler, M. Perryman, A. Andrady, R. Narayan and K. Lavendar Law, *Science*, 2015, **347**, 768–771.
9 C. Wang, J. Zhao and B. Xing, *J. Hazard. Mater.*, 2021, **407**, 124357.
10 L. Su, X. Xiong, Y. Zhang, C. Wu, X. Xu, C. Sun and H. Shi, *Sci. Total Environ.*, 2022, **831**, 154884.
11 A. J. Nihart, M. A. Garcia, E. El Hayek, R. Liu, M. Olewine, J. D. Kingston, E. F. Castillo, R. R. Gullapalli, T. Howard, B. Bleske, J. Scott, J. Gonzalez-Estrella, J. M. Gross, M. Spilde, N. L. Adolphi, D. F. Gallego, H. S. Jarrell, G. Dvorscak, M. E. Zuluaga-Ruiz, A. B. West and M. J. Campen, *Nat. Med.*, 2025, **31**, 1114–1119.
12 D.-W. Lee, J. Jung, S. Park, Y. Lee, J. Kim, C. Han, H.-C. Kim, J. H. Lee and Y.-C. Hong, *Sci. Rep.*, 2024, **14**, 30419.
13 L. C. Jenner, J. M. Rotchell, R. T. Bennett, M. Cowen, V. Tentzeris and L. R. Sadofsky, *Sci. Total Environ.*, 2022, **831**, 154907.
14 T. Rocha-Santos and A. C. Duarte, *TrAC, Trends Anal. Chem.*, 2015, **65**, 47–53.
15 W. Joon Shim, S. Hee Hong and S. Eo Eo, *Anal. Methods*, 2017, **9**, 1384–1391.
16 V. N. de Ruijter, P. E. Redondo-Hasselerharm, T. Gouin and A. A. Koelmans, *Environ. Sci. Technol.*, 2020, **54**, 11692–11705.
17 J. C. Prata, V. Reis, J. P. da Costa, C. Mouneyrac, A. C. Duarte and T. Rocha-Santos, *J. Hazard. Mater.*, 2021, **403**, 123660.
18 S. M. Brander, V. C. Renick, M. M. Foley, C. Steele, M. Woo, A. Lusher, S. Carr, P. Helm, C. Box, S. Cherniak, R. C. Andrews and C. M. Rochman, *Appl. Spectrosc.*, 2020, **74**, 1099–1125.
19 N. R. Jones, A. M. de Jersey, J. L. Lavers, T. Rodemann and J. Rivers-Auty, *J. Hazard. Mater.*, 2024, **465**, 133276.
20 C. Scopetani, M. Esterhuizem-Londt, D. Chelazzi, A. Cincinelli, H. Setälä and S. Pflugmacher, *Ecotoxicol. Environ. Saf*, 2020, **189**, 110036.
21 R. Dris, J. Gasperi, M. Saad, C. Mirande and B. Tassin, *Mar. Pollut. Bull.*, 2016, **104**, 290–293.
22 T. A. Plee and C. M. Pomory, *Mar. Pollut. Bull.*, 2020, **158**, 111437.
23 C. Gwinnett and R. Z. Miller, *Mar. Pollut. Bull.*, 2021, **173**, 113095.

24 R. Bai, R. Fan, C. Xie, Q. Liu, Q. Liu, C. Yan, J. Cui and W. He, *J. Hazard. Mater.*, 2023, **459**, 132068.
25 C. Wesch, A. M. Elert, M. Wörner, U. Braun, R. Klien and M. Paulus, *Sci. Rep.*, 2017, **7**, 5424.
26 G. Kutralam-Muniasamy, V. C. Shruti, F. Pérez-Guevara, P. D. Roy and I. Elizalde-Martínez, *Sci. Total Environ.*, 2023, **875**, 162610.
27 K. Munno, A. L. Lusher, E. C. Minor, A. Gray, K. Ho, J. Hankett, C.-H. T. Lee, S. Primpke, R. E. McNeish, C. S. Wong and C. Rochman, *Chemosphere*, 2023, **333**, 138883.
28 M. J. Noonan, N. Grechi, C. L. Mills and M. A. M. M. Ferraz, *Microplast. Nanoplast.*, 2023, **3**, 17.
29 W. Wang and J. Wang, *TrAC, Trends Anal. Chem.*, 2018, **108**, 195–202.
30 X. Lin, A. A. Gowan, H. Pu and J.-L. Xu, *Food Control*, 2023, **153**, 109939.
31 L. J. Zantis, E. L. Carroll, S. E. Nelms and T. Bosker, *Environ. Pollut.*, 2021, **269**, 116142.
32 B. Nayebi, P. Khurana, R. Pulicharla, S. Karimpour and S. Kaur Brar, *Environ. Sci.: Adv.*, 2023, **2**, 1060–1081.
33 J. Huang, H. Chen, Y. Zheng, Y. Yang, Y. Zhang and B. Gao, *Chem. Eng. J.*, 2021, **425**, 131870.
34 W. J. Gee, *Forensic Sci. Int.*, 2023, **353**, 111874.
35 M. F. Sovinski, *Contamination of Critical Surfaces from NVR Glove Residues via Dry Handling and Solvent Cleaning*, NASA/TM-2004-212752, National Aeronautics and Space Administration, Goddard Space Flight Center, Greenbelt, MD, 2004.
36 M. Garçon, L. Sauzéat, R. W. Carlson, S. B. Shirey, M. Simon, V. Balter and M. Boyet, *Geostand. Geoanal. Res.*, 2016, **41**, 367–380.
37 B. R. Stohmeier, A. Plasencia and J. D. Piasecki, *Spectroscopy*, 2012, **27**, 36–44.
38 C. S. Witzig, C. Földi, K. Wörle, P. Habermehl, M. Pittroff, Y. K. Müller, T. Lauschke, P. Fiener, G. Dierkes, K. P. Freier and N. Zumbülte, *Environ. Sci. Technol.*, 2020, **54**, 12164–12172.
39 A. Carabello, R. Henker and W.-G. Drossel, *Curr. Dir. Biomed. Eng.*, 2022, **8**, 384–387.
40 A. B. Swanson, I. B. Matev and G. de Groot, *Bull. Prosthet. Res.*, 1970, **10**, 145–153.
41 P. K. Ng, M. C. Bee, A. Saptari and N. A. Mohamad, *Theor. Issues Ergon. Sci.*, 2013, **15**, 517–533.
42 C. W. Nicolay and A. L. Walker, *Int. J. Ind. Ergon.*, 2005, **35**, 605–618.
43 R. L. Parham, A. M. Ayala, L. Meagher, M. E. Clough, E. Ochoa Rivera, J. H. Shi, A. Tewari, A. J. McNeil and A. P. Ault, *Anal. Chem.*, 2025, **97**, 18136–18143.
44 J. Brandt, F. Fischer, E. Kanaki, K. Enders, M. Labrenz and D. Fischer, *Front. Environ. Sci.*, 2021, **8**, 579676.
45 G. Renner, A. Nellessen, A. Schwiers, M. Wenzel, T. C. Schmidt and J. Schram, *TrAC, Trends Anal. Chem.*, 2019, **111**, 229–238.
46 M. E. Clough, E. Ochoa Rivera, R. L. Parham, A. P. Ault, P. M. Zimmerman, A. J. McNeil and A. Tewari, *Environ. Sci. Technol.*, 2024, **58**, 21740–21749.
47 J. Weisser, T. Pohl, M. Heinzinger, N. P. Ivleva, T. Hofmann and K. Glas, *TrAC, Trends Anal. Chem.*, 2022, **148**, 116535.
48 L. Cabernard, L. Roscher, C. Lorenz, G. Gerdts and S. Primpke, *Environ. Sci. Technol.*, 2018, **52**, 13279–13288.
49 S. Primpke, P. A. Dias and G. Gerdts, *Anal. Methods*, 2019, **11**, 2138–2147.
50 N. P. Ivleva, *Chem. Rev.*, 2021, **121**, 11886–11936.
51 D. Schymanski, B. E. Oßmann, N. Benismail, K. Boukerma, G. Dallmann, E. von der Esch, D. Fischer, F. Fischer, D. Gilliland, K. Glas, T. Hofmann, A. Käppler, S. Lacorte, J. Marco, M. E. L. Rakwe, J. Weisser, C. Witzig, N. Zumbülte and N. P. Ivleva, *Anal. Bioanal. Chem.*, 2021, **413**, 5969–5994.
52 M. G. J. Löder, M. Kuczera, S. Mintenig, C. Lorenz and G. Gerdts, *Environ. Chem.*, 2015, **12**, 563–581.
53 J. Delgado-Gallardo, G. L. Sullivan, P. Esteban, Z. Wang, O. Arar, L. Zi, T. M. Watson and S. Sarp, *ACS ES&T Water*, 2021, **1**, 748–764.
54 V. Vovk, A. Gammerman, and C. Saunders, *Proceedings of the Sixteenth International Conference on Machine Learning*, Bled, 1999.
55 V. Vovk, A. Gammerman and G. Shafer, *Algorithmic Learning in a Random World*, Springer, New York, NY, 2005.
56 Ansell Nitrilite™ 93-401, https://www.ansell.com/us/en/products/nitrilite-93-401, accessed 2025-04-01.
57 R. Amorese, personal communication.
58 W. Cowger, Z. Steinmentz, A. Gray, K. Munno, J. Lynch, H. Hapich, S. Primpke, H. De Frond, C. Rochman and O. Herodotou, *Anal. Chem.*, 2021, **93**, 7543–7548.
59 W. Cowger, A. Gray, S. H. Christiansen, H. DeFrond, A. D. Deshpande, L. Hemabessiere, E. Lee, L. Mill, K. Munno, N. E. Ossmann, M. Pittroff, C. Rochman, G. Sarau, S. Tarby and S. Primpke, *Appl. Spectrosc.*, 2020, **74**, 989–1010.
60 M. Kooi and A. A. Koelmans, *Environ. Sci. Technol. Lett.*, 2019, **6**, 551–557.
61 R. C. Hale, M. E. Seeley, M. J. La Guardia, L. Mai and E. Y. Zeng, *J. Geophys. Res.: Oceans*, 2020, **125**, e2018JC014719.
62 L. Zhu, Y. Kang, M. Ma, Z. Wu, L. Zhang, R. Hu, Q. Xu, J. Zhu, X. Gu and L. An, *Sci. Total Environ.*, 2024, **915**, 170004.
63 I. Raluca Comnea-Stancu, K. Wieland, G. Ramer, A. Schwaighofer and B. Lendl, *Appl. Spectrosc.*, 2017, **71**, 939–950.
64 J.-K. Park, S. Lee, A. Park and S.-J. Baek, *Anal. Chem.*, 2020, **92**, 10291–10299.
65 J. Lim, J. Seo and D. Shin, *Anal. Chem.*, 2025, **97**, 18432–18443.
66 P. H. R. Ng, S. Walker, M. Tahtouh and B. Reedy, *Anal. Bioanal. Chem.*, 2009, **394**, 2039–2048.
67 G. Renner, T. C. Schmidt and J. Schram, *Anal. Chem.*, 2017, **89**, 12045–12053.
68 J.-K. Park, A. Park, S. K. Yang, S.-J. Baek, J. Hwang and J. Choo, *Analyst*, 2017, **142**, 380–388.
69 D. Prezgot, M. Chen, Y. Leng, L. Gaburici and S. Zou, *Anal. Chem.*, 2025, **97**, 8833–8840.

70 R. Zhang, Z. Shang, S. Lu, N. Jia, X. Jiang, Z. Pu, Y. Du and Y. Hu, *Chemom. Intell. Lab. Syst.*, 2021, **215**, 104353.
71 E. Syranidou, K. Karkanorachaki, D. Barouta, E. Papadaki, D. Moschavos, A. Avgeropoulos and N. Kalogerakis, *Environ. Sci. Technol.*, 2023, **57**, 8130–8138.
72 J. J. Hermans, K. Keune, A. van Loon, M. J. N. Stols-Wilcox, R. W Corkery, and P. D. Iedema, *Proceedings of ICOM-CC 17th Triennial Conference*, Melbourne, Australia, 2014.
73 W. Yagoubi, A. Abdelhafidi, M. Sebaa and S. F. Chabira, *Polym. Test.*, 2015, **44**, 37–48.
74 G. Grause, M.-F. Chien and C. Inoue, *Polym. Degrad. Stab.*, 2020, **181**, 109364.
75 L. Robinet and C. M. Corbiel, *Stud. Conserv.*, 2003, **48**, 23–40.
76 M. de Veij, P. Vandenabeele, T. De Beer, J. P. Remon and L. Moens, *J. Raman Spectrosc.*, 2009, **40**, 297–307.
77 V. Nava, M. L. Frezzotti and B. Leoni, *Appl. Spectrosc.*, 2021, **75**, 1341–1357.
78 G. R. Strobl and W. Hagedorn, *J. Polym. Sci.*, 1978, **16**, 1181–1193.
79 M. Ibrahim, H. He, and R. Chen, *In Situ Density Determination of Polyethylene in Multilayer Polymer Films Using Raman Microscopy*, AN53001_E 03/18M, Thermo Fisher Scientific, Madison, WI, 2018.
80 M. Ibrahim, and H. He, *Classification of Polyethylene by Raman Spectroscopy*, AN52301_E 08/22M, Thermo Fisher Scientific, Madison, WI, 2022.
81 G. Binda, G. Kalčíková, I. John Allan, R. Hurley, E. Rødland, D. Spanu and L. Nizzetto, *TrAC, Trends Anal. Chem.*, 2024, **172**, 117566.
82 S. Phan, J. L. Padilla-Gamiño and C. K. Luscombe, *Polym. Test.*, 2022, **116**, 107752.